

Observation of off-diagonal geometric phases in polarized-neutron-interferometer experiments

Y. Hasegawa,¹ R. Loidl,² G. Badurek,¹ M. Baron,² N. Manini,³ F. Pistolesi,^{4,*} and H. Rauch¹

¹Atominstytut der Österreichischen Universitäten, Stadionallee 2, A-1020 Wien, Austria

²Institut Laue Langevin, Boîte Postale 156, F-38042 Grenoble Cedex 9, France

³Dipartimento di Fisica, Università di Milano, Via Celoria 16, I-20133 Milano, Italy
and INFN, Unità di Milano, Milano, Italy

⁴European Synchrotron Radiation Facility, Boîte Postale 220, F-38043, Grenoble, France

(Received 13 December 2001; published 24 April 2002)

Off-diagonal geometric phases acquired in the evolution of a spin-1/2 system have been investigated by means of a polarized neutron interferometer. Final counts with and without polarization analysis enable us to observe simultaneously the off-diagonal and diagonal geometric phases in two detectors. We have quantitatively measured the off-diagonal geometric phase for noncyclic evolutions, confirming the theoretical predictions. We discuss the significance of our experiment in terms of geometric phases (both diagonal and off-diagonal) and in terms of the quantum-erasing phenomenon.

DOI: 10.1103/PhysRevA.65.052111

PACS number(s): 03.65.Vf, 03.75.Dg, 42.50.-p, 07.60.-j

I. INTRODUCTION

Consider the dynamics of a quantum system governed by a parametrized Hamiltonian. When the parameter is varied along a curve, a normalized eigenstate, with energy eigenvalue $E(s)$, acquires, in addition to the standard dynamical phase given by $\exp[(-i/\hbar)\int E(s)ds]$, a phase factor. This extra phase is called “geometric,” since it is independent of the Hamiltonian, of the energy of the eigenstate, and of the rate of the evolution, and depends only on the sequence of quantum states. This geometric phase was observed by Pancharatnam in an interference experiment with polarized light in the 1950s [1]. Berry then formulated the geometric phase for adiabatic transport along a closed curve (i.e., cyclic evolution [2]), attracting considerable interest [3]. The concept of the geometric phase introduced by Berry was generalized, for instance, to nonadiabatic [4] and noncyclic [5] evolutions. Many experiments in a wide range of physical phenomena were reported to determine the geometric phase [3]: in particular, the geometric phase for the most basic and fundamental example, the two-level system constituted by the neutron spin 1/2, was measured in early neutron experiments [6,7]. The geometric phase can play an important role in quantum-information processing: a controlled phase gate, which requires conditional quantum dynamics, was demonstrated in a nuclear magnetic resonance experiment with the use of a conditional geometric phase [8,9].

The Berry-Pancharatnam geometric phase is the phase of the scalar product of the parallel-transported initial and final states $\langle \Psi^{\parallel}(s_1) | \Psi^{\parallel}(s_2) \rangle$ [2,10]. It may happen that the parallel-transported state is orthogonal to the initial state: in this case the geometric phase is undefined. Recently, the concept of the geometric phase has been extended to the phase factors coming from *cross* scalar products $\langle \Psi_j(s_1) | \Psi_k(s_2) \rangle$

of nondegenerate eigenstates $|\Psi_i\rangle$ [11]. The phase of suitable combinations of these cross products turns out to be a well-defined geometric object, even when the conventional “diagonal” geometric phase is undefined. With respect to diagonal products, these cross products carry complementary geometric information on the evolution and, accordingly, such geometric phases have been termed “off-diagonal.” This formalism was applied successfully to a deformed-microwave-resonator experiment [12,13].

Neutron optical experiments, based on interference of matter waves, have provided elegant demonstrations of the foundations of quantum mechanics [14,15]. In particular, neutron-interferometry experiments have made an impact for more than two decades [16–19]. Among them, those with a polarized incident beam served as an ideal tool to investigate properties of a spin-1/2 system [20]. For instance, starting from spinor superposition [21,22], double-resonance flipper experiments [23], geometric and dynamical phase measurements [24,25], and noncyclic Pancharatnam phase measurement [26] were accomplished. In addition to the interferometric method, the geometric and dynamical phases are more precisely measured with the use of a neutron polarimeter [27]. A neutron interferometer with coupled interference loops was used to create and to measure the spin-independent geometric phase in a sort of double-slit experiment [28].

In this paper, we describe a neutron-interferometric experiment that clearly exhibits and quantitatively measures the off-diagonal geometric phase acquired by noncyclic spinor evolutions of a spin-1/2 system. An incident polarized neutron beam splits into two beam paths and each spinor is rotated to induce appropriate spinor evolutions. With the help of a polarization analysis, the noncyclic off-diagonal geometric phase emerges straightforwardly as the shift of the intensity modulation, whereas the measurement without polarization analysis allows the observation of the diagonal geometric phase, i.e., the noncyclic Pancharatnam phase. Our data confirm theoretical predictions on the off-diagonal geometric phase, illustrating its role for generic evolution and its special significance when the diagonal geometric phase is undefined. In addition, we discuss the quantum-

*Present address: Laboratoire de Physique et Modélisation des Milieux Condensés, Centre National de la Recherche Scientifique, B.P. 166, F-38042 Grenoble Cedex 9, France.

eraser phenomenon for these experiments. A brief report of part of the experimental results has been published previously [29].

II. PRINCIPLE OF THE EXPERIMENT

A. Off-diagonal geometric phase of spin-1/2 system

Consider two nonorthogonal quantum states $|\Psi_I\rangle$ and $|\Psi_{II}\rangle$. The standard interferometric way to measure the phase γ of the scalar product $\langle\Psi_I|\Psi_{II}\rangle = \exp(i\gamma)|\langle\Psi_I|\Psi_{II}\rangle|$ is to superpose the two states, inserting a controlled extra phase factor $\exp(i\chi)$:

$$|\Psi\rangle = \exp(i\chi)|\Psi_I\rangle + |\Psi_{II}\rangle. \quad (1)$$

The resulting interfering intensity

$$I = \langle\Psi|\Psi\rangle = \langle\Psi_I|\Psi_I\rangle + \langle\Psi_{II}|\Psi_{II}\rangle + 2|\langle\Psi_I|\Psi_{II}\rangle|\cos(\chi - \gamma) \quad (2)$$

oscillates as a function of the phase angle χ . The offset of the cosine oscillation of I measures γ , and the amplitude of these oscillations measures the overlap $|\langle\Psi_I|\Psi_{II}\rangle|$.

The basic interferometric concept sketched here can be applied to compare states evolving in time according to a given dynamics. The most basic quantum system is an $S = 1/2$ spinor. In this paper we use neutron interferometry to measure the phases acquired by the neutron spin state precessing under the action of suitably arranged magnetic fields and polarizers. A beam of neutrons initially in a pure $|\Psi^+\rangle = \begin{bmatrix} \cos(\theta/2) \\ \sin(\theta/2) \end{bmatrix}$ polarization state is split and, along the two paths, undergoes different transformations represented by two linear operators A and B (represented by 2×2 unitary matrices), before the two phase-coherent beams $|\Psi_I\rangle = A|\Psi^+\rangle$ and $|\Psi_{II}\rangle = B|\Psi^+\rangle$ are brought together at the final counter.

By choosing A and B suitably in the setup it is possible to measure the recently proposed off-diagonal geometric phase [11] for the evolution of two states according to a given unitary evolution operator U . The off-diagonal phase factor is defined by

$$\exp(i\gamma_{+-}^{\text{off}}) = \Phi(\langle\Psi^+|U|\Psi^-\rangle\langle\Psi^-|U|\Psi^+\rangle), \quad (3)$$

where $\Phi(z) = z/|z|$, $|\Psi^-\rangle = \begin{bmatrix} -\sin(\theta/2) \\ \cos(\theta/2) \end{bmatrix}$ is the spinor orthogonal to $|\Psi^+\rangle$, and U is the unitary operator representing the

evolution of the states *according to parallel transport*. Specifically, $U = U(s_2)$ governs the evolution $|\Psi^\pm(s)\rangle$ of $|\Psi^\pm\rangle$ to the final value s_2 of the evolution parameter s , according to

$$|\Psi^\pm(s)\rangle = U(s)|\Psi^\pm\rangle, \quad (4)$$

with the parallel transport condition on the phases along the evolution such that the following equation holds:

$$\langle\Psi^\pm(s)|\nabla_s|\Psi^\pm(s)\rangle = 0. \quad (5)$$

In this way, the (nongeometric) dynamical phase vanishes identically along the evolution. The choice of A and B that permits one to measure γ_{+-}^{off} interferometrically is the following:

$$A = P(|\Psi^-\rangle)U^{-1}, \quad B = P(|\Psi^-\rangle)U, \quad (6)$$

where $P(|\Psi^-\rangle) = |\Psi^-\rangle\langle\Psi^-|$ is a projection operator (representing a neutron spin polarizer), and U^{-1} is the reversed evolution with respect to U .

In the present work, we consider only precessions around the \hat{z} direction, determining a unitary time evolution

$$U(t) = \begin{bmatrix} \exp\left(\frac{i\omega_L t}{2}\right) & 0 \\ 0 & \exp\left(-\frac{i\omega_L t}{2}\right) \end{bmatrix}, \quad (7)$$

where ω_L is the Larmor frequency: with this special choice, spinors restricted to the \hat{x} - \hat{y} plane ($\theta = \pi/2$) are parallel transported by U . In addition, even for ($\theta \neq \pi/2$), the extra dynamic phases $\Phi_D^+ = -\Phi_D^- = (\omega_L t/2)\cos\theta$ introduced by U happen to cancel exactly in the product (3), and are therefore immaterial for γ_{+-}^{off} .

Under the action of this choice of evolution operators, the expected intensity

$$I = \|\exp(i\chi)|\Psi_I\rangle + |\Psi_{II}\rangle\|^2 \quad (8)$$

can be computed in accordance with Eq. (2). Applying explicitly the unitary evolution U of Eq. (7), the interfering states $|\Psi_I\rangle = P(|\Psi^-\rangle)U^{-1}|\Psi^+\rangle = i\sin(\theta)\sin(\omega_L t/2)|\Psi^-\rangle$ and $|\Psi_{II}\rangle = P(|\Psi^-\rangle)U|\Psi^+\rangle = -|\Psi_I\rangle$ combine to give

$$\begin{aligned} I &= \langle\Psi^+|U|\Psi^-\rangle\langle\Psi^-|U^{-1}|\Psi^+\rangle + \langle\Psi^+|U^{-1}|\Psi^-\rangle\langle\Psi^-|U|\Psi^+\rangle + 2\text{Re}[\exp(i\chi)\langle\Psi^+|U|\Psi^-\rangle\langle\Psi^-|U|\Psi^+\rangle] \\ &= 2\sin^2(\theta)\sin^2(\omega_L t/2) - 2\sin^2(\theta)\sin^2(\omega_L t/2)\cos(\chi) \\ &= 2\sin^2(\theta)\sin^2(\omega_L t/2)[1 + \cos(\chi - \pi)]. \end{aligned} \quad (9)$$

This derivation illustrates that the inverse evolution U^{-1} fulfills the role of eliminating all U dependence [apart from a global factor $\sin^2(\omega_L t/2)$] in the noninterfering amplitude, while letting the phases of the off-diagonal matrix elements of U combine in the correct way to have the off-diagonal

geometric phase γ_{+-}^{off} of Eq. (3) as a shift in the interfering amplitude.

The comparison of Eqs. (9) and (2) indicates that $\gamma_{+-}^{\text{off}} = \pi$, an equation representing the phase relation $|\Psi_{II}\rangle = -|\Psi_I\rangle$. We have recovered here the result of Ref. [11],

where it was shown that for *any* evolution (not necessarily restricted to precessions around the \hat{z} direction) the off-diagonal phase γ_{+-}^{off} of the two-state system must equal π . This is a consequence of the relatively restrict dynamics of the two-state system. Systems with a larger number of degrees of freedom are expected to show a more intricate pattern of diagonal and off-diagonal phases, depending explicitly on the states considered and on the evolution path.

B. Experimental strategy with the use of the neutron interferometer

Equation (8) describes mathematically the following experiment. A neutron beam, fully polarized to the incident spinor $|\Psi^+\rangle$, is split (the two terms sum); then appropriate spinor rotations U and U^{-1} , in addition to the auxiliary phase shift of χ , act on the two paths. The two beams are brought together and finally the intensity is measured with the polarization analysis orthogonal to the incident spinor (the projector factor). The unitary evolution is realized by the magnetic field in the $+\hat{z}$ direction. The inverse precession U^{-1} is simply obtained by applying a reversed field to one of the two arms of the interferometer.

We draw the reader's attention to the fact that, when the spin analysis is not performed ($A=U, B=U^{-1}$), Eq. (8) reduces to

$$\begin{aligned} I &= \|\exp(i\chi)U^{-1} + U\|\Psi^+\|^2 \\ &= \|\exp(i\chi) + U(2t)\|\Psi^+\|^2. \end{aligned} \quad (10)$$

This exhibits another possibility for observing the diagonal part of the geometric phase, i.e., the noncyclic Pancharatnam phase, simply by bypassing the final spin analysis in the experiment. Note, however, the presence of $U(2t) = UU = U^2$ in Eq. (10), indicating that the measured phase refers to a path undergoing *twice* the precession angle experienced by the actual neutron spin of either split beam.

C. Poincaré sphere description

A completely general geometric interpretation of the off-diagonal geometric phase was given in Ref. [11] in terms of geodesic (shortest path connecting two points, associated with null geometric phase) in the projective space. The off-diagonal geometric phase γ_{jk}^{Γ} can be represented as an integral over the surface bounded by the four paths Γ_j (trajectory of the state $|\Psi_j\rangle$) + G_{jk} [geodesic path from $|\Psi_j(\mathbf{s}_2)\rangle$ to $|\Psi_k(\mathbf{s}_1)\rangle$] + Γ_k (trajectory of the state $|\Psi_k\rangle$) + G_{kj} [geodesic from $|\Psi_k(\mathbf{s}_2)\rangle$ to $|\Psi_j(\mathbf{s}_1)\rangle$]; similarly, the diagonal geometric phase, for instance γ_j^{Γ} , is given by a surface enclosed by the two paths $\Gamma_j + G_{jj}$ [geodesic from $|\Psi_j(\mathbf{s}_2)\rangle$ to $|\Psi_j(\mathbf{s}_1)\rangle$].

In the special case at hand of a two-state system, the projective space is conveniently represented by the Poincaré (unit) sphere, for two main reasons. First, this mapping carries over the metric so that any projective geodesic is mapped on a spherical geodesic, i.e., the shortest path connecting two points. Second, the integral [2] over the surface bounded by a closed path in projective space that gives the geometrical phase acquired along such a path reduces simply

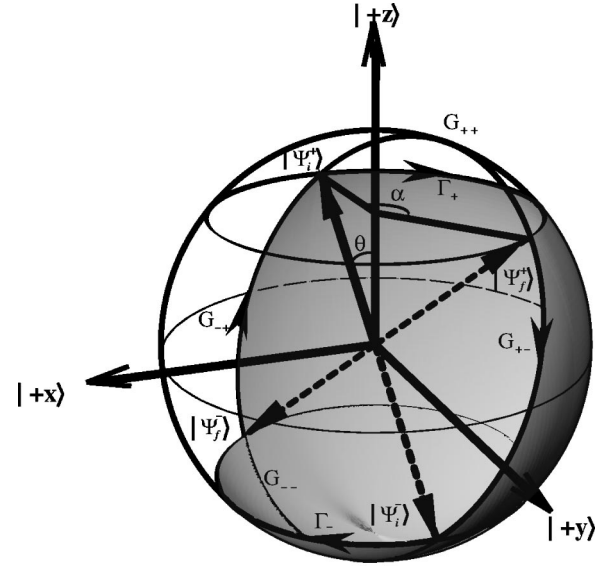


FIG. 1. Schematic representation of the spinor evolution on the Poincaré sphere to illustrate the off-diagonal geometric phase. $|\Psi_i^+\rangle$ evolves to $|\Psi_f^+\rangle$ with the corresponding orthogonal states $|\Psi_i^-\rangle$ to $|\Psi_f^-\rangle$. All states and geodesics are in one plane. The shaded surface corresponds to the off-diagonal geometric phase. Its 2π solid angle yields a phase shift of π .

to twice the geometric surface enclosed by the loop on the Poincaré sphere.

Initially, we take the incident spinor $|\Psi^+\rangle$ pointing in a direction tilted by θ from $+\hat{z}$ in the \hat{z} - \hat{y} plane, and then let a magnetic field parallel to \hat{z} rotate it by an angle $\alpha = \omega_L t$. The orthogonal spinor $|\Psi^-\rangle$ points the opposite way at each time along the evolution. In Fig. 1 we represent the initial spinor $|\Psi_i^+\rangle = |\Psi^+\rangle$ (bold solid arrow) evolving to $|\Psi_f^+\rangle$ (bold dashed arrow) under the action of the magnetic field, thus defining the trajectory Γ_+ . The diametrically opposed evolution of $|\Psi^-(t)\rangle$ from $|\Psi_i^-\rangle$ to $|\Psi_f^-\rangle$ gives the trajectory Γ_- . For any α , the initial and final states lie in a unique plane, except in the special case $\alpha = 0^\circ \text{ mod } 360^\circ$, for which γ_{+-}^{Γ} is undefined, since the off-diagonal elements of U vanish. For any other value of α , the geodesics G_{+-} and G_{-+} indicated in Fig. 1 are uniquely determined.

The shaded area surrounded by Γ_+ , G_{+-} , Γ_- , and G_{-+} equals one-half of the off-diagonal geometric phase. By recognizing the equivalence of the shaded area with the half sphere surrounded by the sequence of the four geodesic paths G_{++} , G_{+-} , G_{--} , and G_{-+} , it is clear that this shaded area equals half the spherical surface, i.e., 2π (independently of α). This illustrates the constant value $\gamma_{+-}^{\text{off}} = \pi$ taken by the off-diagonal geometric phase, as discussed in Sec. II A. The Poincaré sphere representation also shows how the off-diagonal geometric phase is especially significant when the diagonal geometric phase is ill defined. The diagonal Berry-Pancharatnam phase γ_+ is represented in Fig. 1 by the spherical sector between Γ_+ and G_{++} . This sector becomes ill defined for $\theta = 90^\circ$ and $\alpha = 180^\circ$, since G_{++} is then arbitrary. Nevertheless, the off-diagonal geometric phase is deduced independently of both geodesics

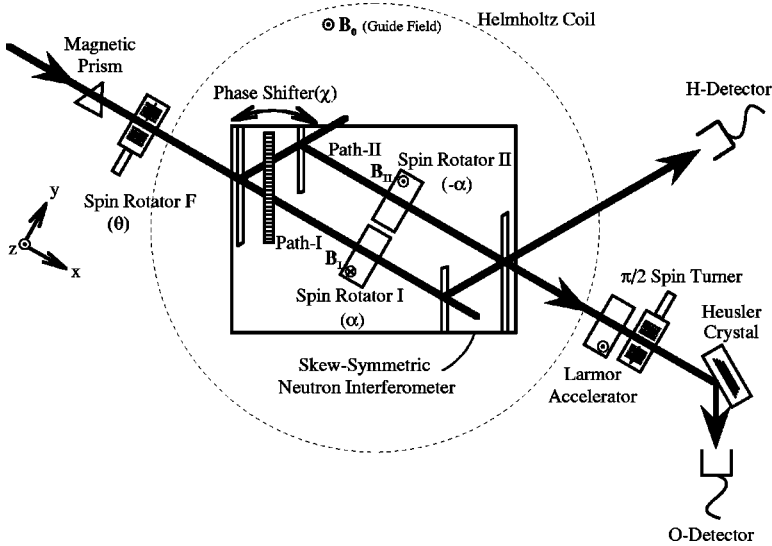


FIG. 2. Schematic view of the experimental setup to observe the off-diagonal geometric phase. An incident polarized neutron beam splits into two beam paths in the interferometer and each spinor is rotated to induce appropriate spinor evolutions. *A posteriori* spin analysis allows the observation of the off-diagonal geometric phase. A measurement without spin analysis reveals the diagonal geometric phase.

G_{++} and G_{--} ; therefore its value remains well defined. Incidentally, in this special case the geodesic paths G_{+-} and G_{-+} reduce to single points.

III. EXPERIMENT

A. Setup

The experiment was carried out at the perfect-crystal-interferometer beamline S18 at the high-flux reactor at the Institut Laue Langevin (ILL) [30]. A schematic view of the experimental setup is shown in Fig. 2. Before falling on a skew-symmetric triple-Laue interferometer, the incident neutron beam was collimated and monochromatized by the 220 Bragg reflection of a Si perfect crystal monochromator placed in the thermal neutron guide H25. The wavelength was tuned to give a mean value $\lambda_0 = 1.92 \text{ \AA}$ ($\Delta\lambda/\lambda_0 \sim 0.02$). This incident beam was slightly separated in angle with the use of the spin-dependent birefringence of neutrons on passing through prismatically shaped magnetic fields oriented in the vertical direction, i.e., perpendicular to the beam trajectory defining \hat{z} [31]. The beam cross section was confined to $8 \times 8 \text{ mm}^2$ and a spin rotator F was inserted to tune the polar angle θ of the incident spinor. The interferometer was adjusted to give 220 reflection in a nondispersive arrangement relative to the monochromator, picking up neutrons polarized in one direction. A pair of water-cooled Helmholtz coils produced a fairly uniform magnetic guide field $B_0 \hat{z}$ across the interferometer. An isothermal box enclosed the interferometer to achieve reasonable thermal environmental isolation. A magnetically saturated Heusler crystal together with a Larmor accelerator and a rectangular spin-1/2 turner enabled spin analysis, i.e., the selection of neutrons with certain polarization directions, for one of the two interfering beams [32]. This O beam was used to observe the phase shift due to the off-diagonal geometric phase. In addition, we measured the intensity of the other interfering (H) beam without spin analysis to show the phase shift due to the diagonal geometric phase.

In order to estimate depolarization, the efficiency of the spinor rotations in the spin-analyzing part, and other imper-

fections of the setup, the interferometer was first adjusted to accept only spin-up polarized neutrons, i.e., $|+z\rangle$, with the spin rotator F turned off. The fraction of the $|+z\rangle$ component was measured to be 0.92 with the use of the spin turner. Since the present measurement demands the polarization of the incident beam to lie in the \hat{x} - \hat{z} plane, the spin rotator F was turned on to tune the polar angle θ of the spin direction. The magnetic guide field was optimized to $B_0 = 18 \text{ G}$ to avoid additional depolarization. The measurement with the use of the Larmor accelerator revealed that the fraction of the desired component was reduced to 0.87, which was still high enough to accomplish the measurements. Nonessential spinor precessions are induced by the guide field all through the beam trajectories. Nevertheless, the commutability between the operators for the essential spinor rotations [U and U^{-1} in Eq. (8)] and the nonessential rotations (introduced by the guide field) allows compensation for these nonessential rotations behind the interferometer, with the use of the Larmor accelerator.

The essential unitary evolutions U and U^{-1} were realized in the experiment by setting the magnetic fields in the two identical spin rotators in an antiparallel direction, i.e., in the $\pm \hat{z}$ directions. In practice, a pair of spin rotators I and II was inserted in the split beam paths. These spin rotators were identical dc coils except for the current directions, i.e., the directions of the induced magnetic fields. They were connected in series to give the same strengths of the magnetic fields in the $\pm \hat{z}$ direction. Each coil was made of an 8-mm-wide and 0.5-mm-thick anodized Al band, where the hydrogen in the insulator was replaced by deuterium to avoid small-angle scattering, would onto a water-cooled Cu frame. These coils induced 180° spinor rotations when operated at 9.8 A, dissipating about 0.6 W each. The rotation angle $\alpha = \omega_L t$ was tuned by adjusting the current and possibly by changing their polarities. Special attention was paid to eliminating both heat and vibration transmission to the interferometer.

Interferograms were obtained in two detectors by rotating a 5-mm-thick parallel-sided Al plate as a phase shifter. The detectors were placed downstream of the interfering O beam

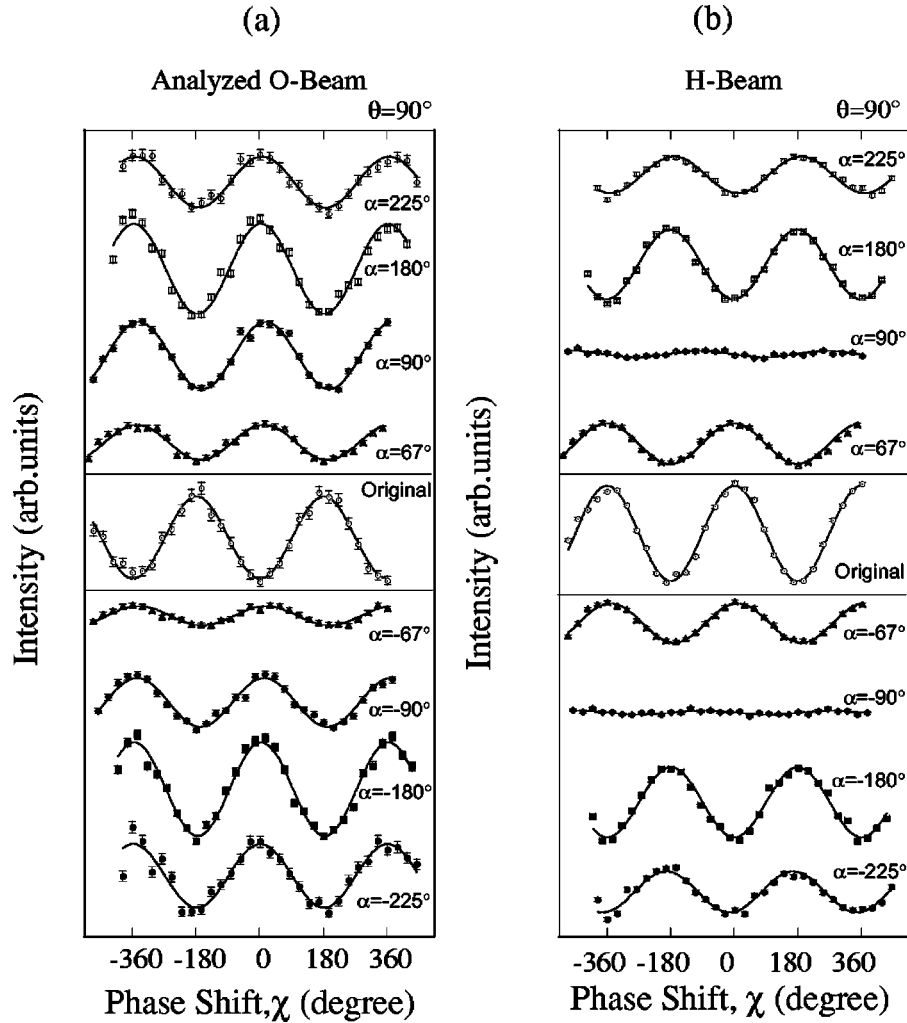


FIG. 3. Typical interferograms for the polar angle of the incident polarization, $\theta=90^\circ$, with various spin rotation angles α . The center figure shows the original ($\alpha=0^\circ$). Curves are least-squares fits. (a) Obtained by the *O* beam with spin analysis. All patterns get a phase shift of 180° with respect to the original when the spinor is rotated, resulting from the off-diagonal geometric phase. (b) Obtained by the *H* beam. The patterns show phase shifts of 0° or 180° . These shifts result from a noncyclic Pancharatnam (diagonal) phase.

in the forward direction behind the spin-analysis system, and directly in the *H* beam in the reflected direction without a spin analysis. These two detectors enabled us to measure simultaneously the properties of the diagonal and off-diagonal geometric phases. For each phase-shifter position, two intensities were measured: typically with the spin rotators I and II turned on (measuring time 10 s), and with the spin rotators turned off (measuring time 20 s). This procedure gave simultaneously two interferograms with and without spinor rotations, thus avoiding instabilities producing undesired phase shifts between the two measurements.

In measuring the interferograms, we determined the phase shift, given by the phase shifter, to have the same value at the same position, when the coils are not activated. In practice, the imperfect polarization of the beam enabled us to record interferograms even for the unaffected beam, i.e., without spinor rotations, where no modulation is expected from the theory. The contrast of the interference oscillations, obtained by the *O* beam, was typically 64% for the empty interferometer, and was reduced to about 40% after inserting the dual

spin rotators. This contrast dropped in some situations to about 30%, mainly due to thermal disturbances. We repeated the same measurements at least three times to ensure that the results were reliable.

B. Interferograms

In the first experiment, the polar angle of the incident polarization was tuned to $\theta=90^\circ$, which shows the most characteristic property of the off-diagonal geometric phase. The spin rotators I and II were tuned to give rotations $\alpha = 45^\circ, \pm 67.5^\circ, \pm 90^\circ, \pm 180^\circ$, and $\pm 225^\circ$. The Larmor accelerator was adjusted so that 180° precession was induced to analyze the spinor orthogonal to the incident one. In addition, the nonessential precession by the guide field was compensated. Figure 3 shows typical interferograms for several spinor rotation angles α , together with the original interferogram ($\alpha=0^\circ$) as a reference. The curves are least-squares fits.

In the interferograms of the *O* beam [Fig. 3(a)], where the off-diagonal geometric phase is expected to appear, all pat-

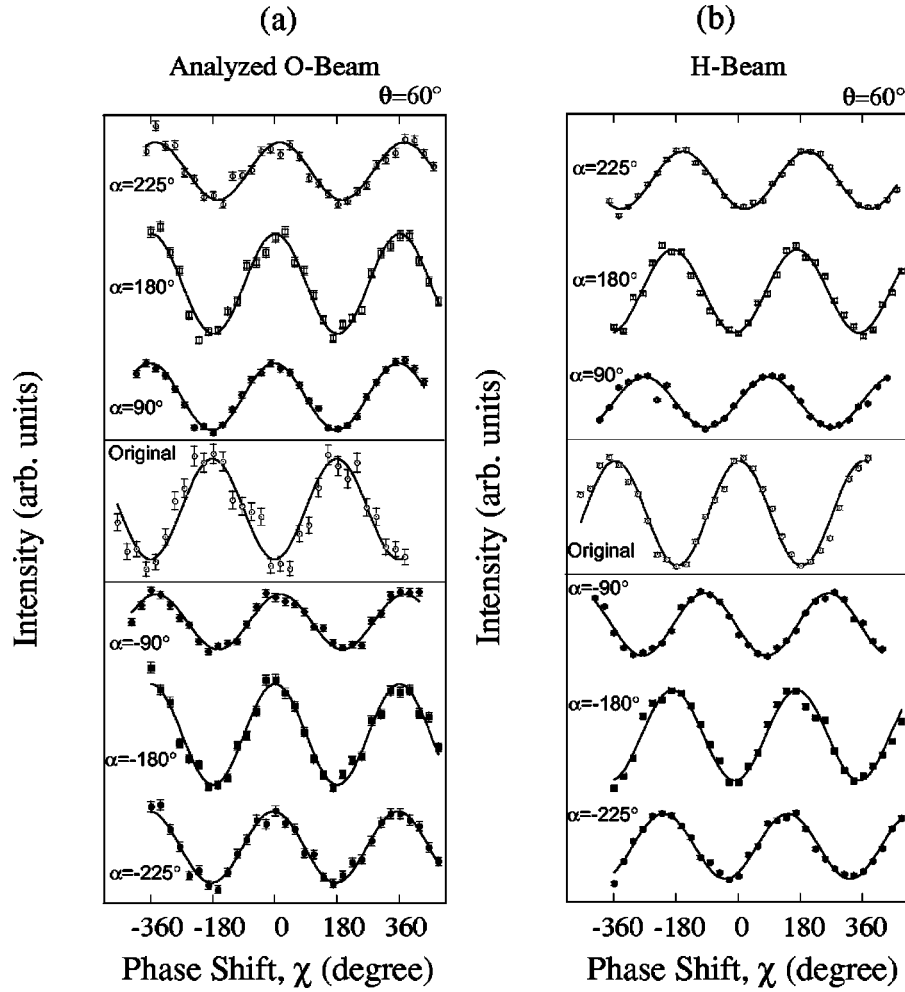


FIG. 4. A series of interferograms for $\theta = 60^\circ$ with various α , accompanied by curves of the least-squares fits. (a) Obtained by the O beam with spin analysis. The patterns get a phase shift of 180° to the original when the spinor is rotated, resulting from the off-diagonal geometric phase. (b) Obtained by the H beam. The patterns get shifted variously, *partly* due to the diagonal geometric phase, or rather due to the noncyclic Pancharatnam phase.

terns with spinor rotations are reflected. This confirms the phase shift of 180° due to the off-diagonal geometric phase. In addition, one sees that the amplitude of the oscillations has its maximum at $\alpha = 180^\circ$ and that it falls gradually when α departs from 180° . This arises from the fact that, with increase of the spinor rotation angle, the orthogonal component to the incident spinor increases until $\alpha = 180^\circ$ and then decreases. In contrast, interferograms of the H beam [Fig. 3(b)] show phase shifts of 0° or 180° . These shifts result from the Pancharatnam phase, or from a noncyclic *pure* diagonal geometric phase, since the dynamical phase or the parallel-transport variant phases Φ_D^\pm are zero in these particular circumstances. It is worth noting here that no interference oscillations emerged when the spinor rotation angle $\alpha = \pm 90^\circ$. In the vicinity of this point, a phase jump from 0° to 180° is expected to occur, which is characteristic for circuits around phase singularities [33]. We will discuss this lack of oscillation in more detail with regard to the significance of the off-diagonal geometric phase as well as the quantum eraser in Sec. IV. In addition, one sees here the sign

changes of the spinor wave function with $\pm 360^\circ$ spinor rotations (i.e., for $\alpha = \pm 180^\circ$), as resulting from the 4π periodicity of the spin-1/2 wave function.

In a second series of measurements, the angle characterizing the incoming polarization was varied, to $\theta = 135^\circ$, 60° , and 30° . At each polar angle, we induced spinor precessions $\alpha = \pm 90^\circ$, $\pm 180^\circ$, and $\pm 225^\circ$. The Larmor accelerator was adjusted to analyze the spinor orthogonal to the incident one. Typical interferograms are shown in Fig. 4 for spinor rotation angle $\alpha = 60^\circ$ together with the original interferogram ($\alpha = 0^\circ$) as a reference. The curves are least-squares fits. Here also, the O beam [Fig. 4(a)] shows a phase shift of 180° due to the off-diagonal geometric phase as the theory predicts, whereas the H beam [Fig. 4(b)] indicates a gradual shift of the oscillations. In this case, this shift is not due to a pure noncyclic diagonal geometric phase, but to a combination of the noncyclic dynamical and geometrical phases, or rather the noncyclic Pancharatnam phase. The sign changes of the spin-1/2 wave functions with $\pm 360^\circ$ spinor rotations, i.e., $\alpha = \pm 180^\circ$, are also seen.

C. Evaluation of off-diagonal geometric phases

In the previous subsection, the variations of the interferograms qualitatively showed the effect of the off-diagonal geometric phase. Here, the noncyclic off-diagonal geometric phase is quantitatively derived from the experimental data. The shift of the oscillations obtained by the O beam is exactly the measure of the off-diagonal geometric phase, when one extracts it as the shift from the original interferogram ($\alpha=0^\circ$). The observed off-diagonal geometric phases at various spinor rotation angles α are plotted for the cases $\theta = 135^\circ, 90^\circ, 60^\circ$, and 30° in Fig. 5. For $\theta=30^\circ$ and $\alpha=90^\circ$, the amplitude of the oscillation was too small to give a reliable value; thus these cases were discarded. The theory predicts a shift of 180° for all cases. The experimental results show good agreement with the theory. Slight deviations from the value of 180° seem systematic, and we suppose them to be due to the imperfect polarization. Theoretical calculations of the off-diagonal geometric phase as should be observed in the experiment, accounting for the effect of the actual polar-

ization, are indicated as dashed lines in Fig. 5. The better agreement between predicted and observed results justifies *a posteriori* these considerations and the experimental results.

IV. DISCUSSION

A. Off-diagonal matrix elements and phases

It is instructive to show the unitary evolution U with the $|\pm z\rangle$ spinor basis, which will clarify the significance of the quality measured in the experiment, i.e., the off-diagonal property. The transformation of the basis from the $|\pm z\rangle$ to the $|\Psi^\pm\rangle$ spinor basis is given in matrix form by

$$T = \begin{bmatrix} \cos\left(\frac{\theta}{2}\right) & \sin\left(\frac{\theta}{2}\right) \\ -\sin\left(\frac{\theta}{2}\right) & \cos\left(\frac{\theta}{2}\right) \end{bmatrix}. \quad (11)$$

With this transformation matrix, the unitary evolution reads

$$U' = TUT^{-1} = \begin{bmatrix} \cos\left(\frac{\omega_L t}{2}\right) + i \cos \theta \sin\left(\frac{\omega_L t}{2}\right) & -i \sin \theta \sin\left(\frac{\omega_L t}{2}\right) \\ -i \sin \theta \sin\left(\frac{\omega_L t}{2}\right) & \cos\left(\frac{\omega_L t}{2}\right) - i \cos \theta \sin\left(\frac{\omega_L t}{2}\right) \end{bmatrix}. \quad (12)$$

Equation (3) yields $\exp[i\{\gamma_{+-}^{\text{off}} + (\Phi_D^- + \Phi_D^+)\}] = \Phi(U'_{-+}U'_{+-})$, and the present experiments measured exactly the value of $\Phi(U'_{-+}U'_{+-})$, which is deduced from the off-diagonal elements of the unitary evolution U' . We recall that in our setup the sum of the dynamical phases, or the parallel-transport variant phases, $\Phi_D^- + \Phi_D^+ = 0$. Therefore, the value $\Phi(U'_{-+}U'_{+-})$, representing the phase of the product of the off-diagonal elements, directly corresponds to the off-diagonal geometric phase γ_{+-}^{off} .

The off-diagonal geometric phase has its greatest importance when the diagonal geometric phase is undefined, i.e., with the 180° spinor rotation in the case of the polar angle of the incident polarization $\theta=90^\circ$. In our setup, the H beam without spin analysis allowed us to observe the diagonal element of the geometric phase only for a doubled spinor rotation angle 2α . Figure 6 shows the intensity modulations in the measurements of the diagonal and off-diagonal geometric phases when the relevant spinor rotation angle is 180° . The modulations of the diagonal and the off-diagonal components were obtained by the H beam with $\alpha = -90^\circ$ and the O beam with $\alpha = -180^\circ$. It is clearly seen that, even when the diagonal one is undefined due to the absence of the oscillation, the off-diagonal geometric phase is defined, and carries the geometrical information associated with the evolution of the state.

B. Quantum erasing

As shown above, both off-diagonal and diagonal geometric phases were recorded with the use of the O beam with

spin analysis and the H beam without spin analysis in our experiment. With respect to wave-particle duality, this spin analysis can modify the path information, yielding a recovery of the interference fringes: this is an example of the so-called quantum eraser [31,34]. We define the quantum eraser here simply as the phenomenon where the wave property, i.e., interference, can be reestablished by modifying the path information in the interfering beam after recombining the beams. This quantum eraser was observed in our experiment, for instance, in the case of $\theta=90^\circ$. Interferograms obtained by the O and H beams are plotted for the spinor rotation angles $\alpha=67^\circ, 90^\circ$, and 180° in Fig. 7. Here, the path information was labeled in the neutron's spin degree of freedom. Thus, the visibilities of the H beam (without spin analysis) were reduced according to the degree of this labeling. In particular, no interference oscillation was exhibited in the case of complete labeling by the orthogonal spinors ($\alpha=90^\circ$). On the contrary, oscillations with visibilities as high as the original (without the spinor rotation) were obtained for the O beam by completely unlabeled the path information with the use of an appropriate spin analysis. This complete modification of the path information, i.e., complete quantum erasing, can also be interpreted as postselection of the subensembles that exhibit perfectly visible fringes from the ensembles with reduced visibility.

C. Alternative geometrical description

The experiment presented in this paper is based on two separate evolutions of a single quantum state. The choice

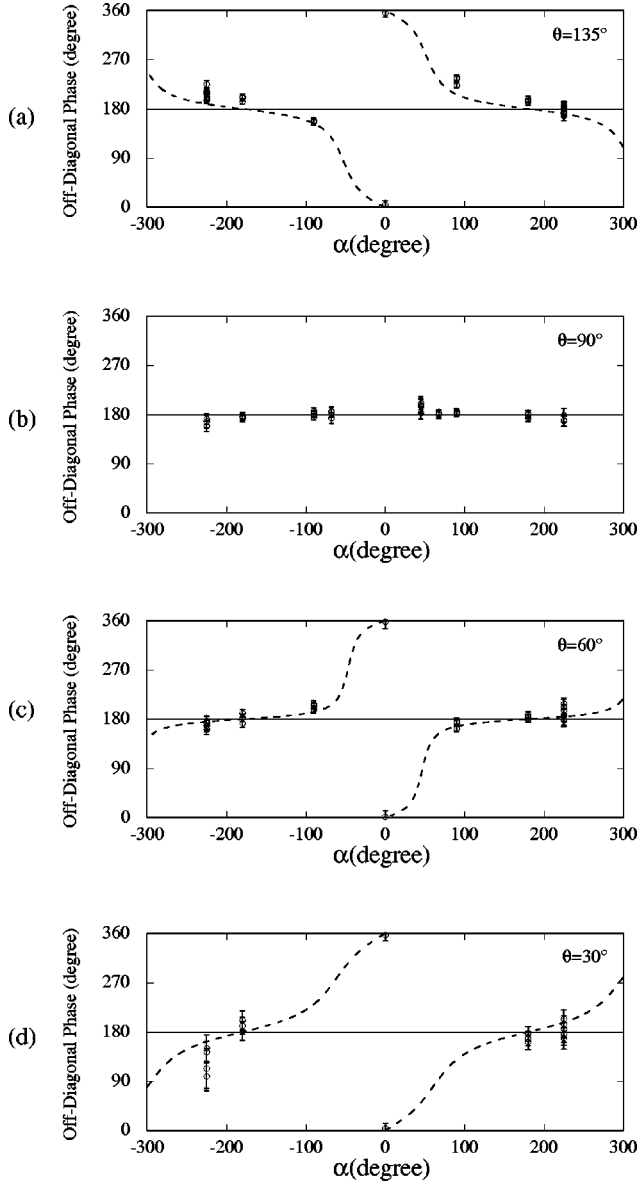


FIG. 5. Observed off-diagonal geometric phase for various polar angles θ of the incident polarization. In the case of an ideal experimental situation, theory predicts the off-diagonal geometric phase of 180° except for the point $\alpha=0^\circ$, where it is undefined. Dashed lines are the theoretical predictions with effective incident polarizations taken into account.

[Eq. (6)] of different evolutions A and B for the state along the two paths is a technical device to measure the inner product (3) yielding the off-diagonal geometric phase of a fictitious system of two spins which evolve under the action of a single unitary dynamics U . Of course, the same measured phase could also be interpreted directly in terms of geometric properties of the actual system under observation. In this section we discuss briefly this alternative interpretation on the Poincaré sphere.

The spectrometer is set up to measure the interference between the two evolved kets

$$|\Psi_I\rangle = A|\Psi^+\rangle = P(|\Psi^-\rangle)U^{-1}|\Psi^+\rangle, \quad (13)$$

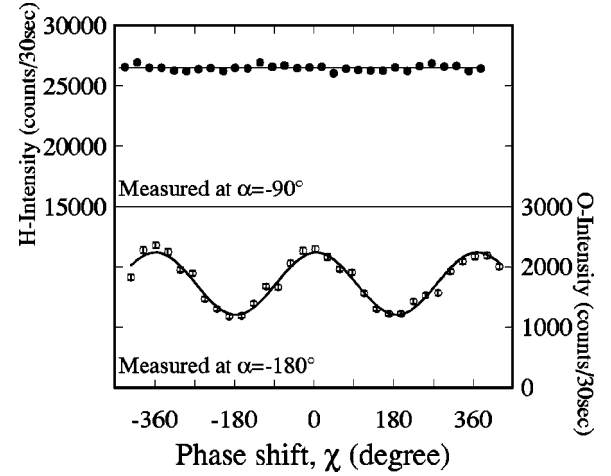


FIG. 6. Intensity modulations obtained by the O and H beams to illustrate the significance of the off-diagonal geometric phase, for 180° spinor rotation. While the H -beam intensity shows no interference oscillations due to the undefined diagonal geometric phase, the O -beam intensity shows a remarkable oscillation since the off-diagonal geometric phases has a definite value.

$$|\Psi_{II}\rangle = B|\Psi^+\rangle = P(|\Psi^-\rangle)U|\Psi^+\rangle. \quad (14)$$

The first (unitary) part of these evolutions is the $\pm\alpha$ precession, represented by the paths Γ_I and Γ_{II} on the Poincaré sphere of Fig. 8. The subsequent projections $P(|\Psi^-\rangle)$ are represented by the geodesic lines G_I and G_{II} . The standard Berry-Pancharatnam geometric phase is usually defined in terms of a single state, which is compared to itself at the beginning of the evolution. That is realized in practice by taking either A or B to be the identity. We consider the straightforward generalization of letting both A and B be the nontrivial operators of Eqs. (13) and (14). The generalized Berry-Pancharatnam geometric phase acquired in this direct (two-state) evolution is therefore

$$\begin{aligned} \exp(i\gamma^{\text{BP}}) &= \Phi(\langle\Psi_{II}|\Psi_I\rangle) \\ &= \Phi(\{\langle\Psi^+|U\rangle|\Psi^-\rangle\langle\Psi^-|\{U|\Psi^+\rangle\}), \end{aligned} \quad (15)$$

where we have put curly brackets in order to indicate the states on which the unitary evolution is originally acting, and have used the fact that $(U^{-1})^\dagger = U$. This geometric phase is represented by the shaded area surrounded by the two paths starting off at $|\Psi^+\rangle$ and rejoining at $|\Psi^-\rangle$ in Fig. 8 (passing through $|\Psi_I\rangle$ and $|\Psi_{II}\rangle$, respectively). In our experimental circumstances, the solid angle bounded by this loop results in $\Omega = 2\pi + 2\alpha \cos\theta$, which translates into a geometric phase $\gamma^{\text{BP}} = (\pi + \alpha \cos\theta)$.

These relations are applicable under the condition that U realizes parallel evolution. However, in our experiment (for $\theta \neq \pi/2$) this is not the case; extra dynamical phases contribute as follows:

$$\begin{aligned} \exp[i(\gamma^{\text{BP}} + \Phi_D^I - \Phi_D^{II})] \\ = \Phi(\{\langle\Psi^+|U\rangle|\Psi^-\rangle\langle\Psi^-|\{U|\Psi^+\rangle\}). \end{aligned} \quad (16)$$

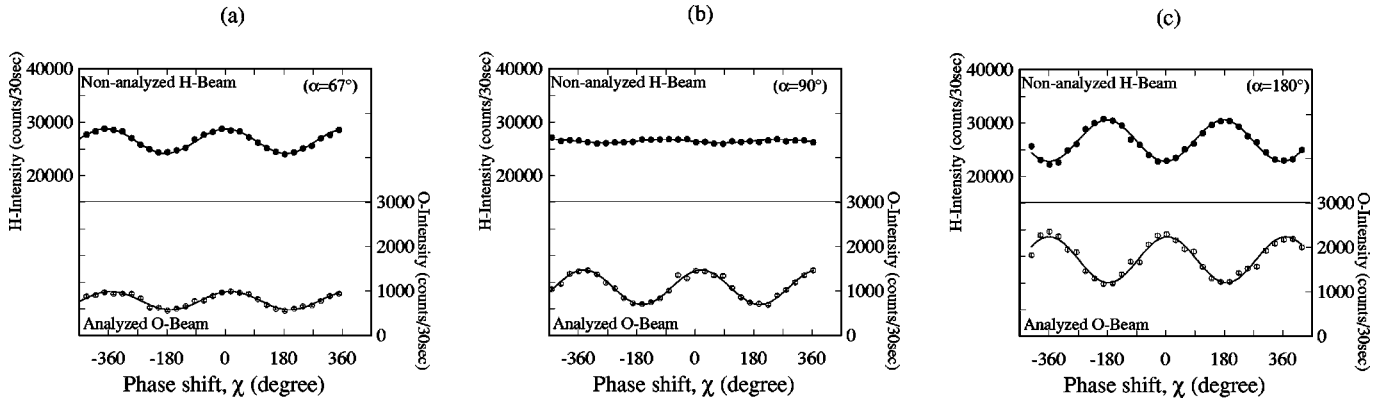


FIG. 7. Intensity modulations obtained by the O and H beams to illustrate a quantum eraser for the polar angle of the incident spinor $\theta=90^\circ$ and spinor rotation angles $\alpha=(a) 67^\circ$, (b) 90° , and (c) 180° . When the path information is labeled in the neutron's spin degree of freedom, the visibilities of the oscillations are reduced (H beam). In contrast, when this labeling is erased with the use of spin analysis, oscillations with high visibilities appear (O beam).

By replacing the values of the dynamical phases $\Phi_D^{II/I} = \pm(\alpha/2)\cos\theta$, we obtain the observed phase difference

$$\gamma^{\text{BP}} + \Phi_D^I - \Phi_D^{II} = (\pi + \alpha \cos\theta) - (\alpha/2)\cos\theta - [-(\alpha/2)\cos\theta] = \pi, \quad (17)$$

which is indeed the value expected for γ_{+-}^{off} .

It is worth noting that the dynamical phase difference for the two evolving states does *not* disappear in this “direct-evolution” interpretation of our experiment. On the contrary, the observed phase γ_{+-}^{off} is interpreted as the combination of a geometrical part γ^{BP} plus a dynamical part $\Phi_D^I - \Phi_D^{II}$. This sheds light on the key mechanism on which our single-interference experiment is based. We remind the reader that the definition of the off-diagonal phase would imply the simultaneous evolution of a *pair* of orthogonal states under the action of the same Hamiltonian: that would in principle require a double-interference experiment [11]. The carefully tailored compensation of the dynamical phases of our experiment eliminates one of the interference conditions, providing a way to measure the off-diagonal phase in terms of the standard interference phase of a spin-1/2 system.

D. Generalizations

The formalism outlined in Sec. II suggests that, in addition to the measurement of “canonical” geometric phases, it should be possible to extend the interferometric technique presented in this work to measure other geometric properties of neutron spin evolutions. The choice (6) is a very special one, strictly constraining the motion of the two spinors to remain orthogonal at all times. This is indeed required to measure the geometric properties of the evolution of the whole set of basis states [here $|\Psi^+(t)\rangle$ and $|\Psi^-(t)\rangle$] according to a single dynamics operator U .

However, one could rightfully let one spinor path evolve under the action of some dynamical operator (for example precession around a \hat{z} -oriented magnetic field), while the other spinor evolves according to a completely different dynamics (an \hat{x} -oriented magnetic field, say). More complex paths on the Poincaré sphere could be investigated by se-

quences of differently oriented magnetic fields. It would be of essential importance to guarantee parallel transport of the states, or a way to explicitly compensate for spurious dynamical phase contributions. If this could be realized, it would be possible to “decouple” the paths of the two spinors on the Poincaré sphere, and thus to investigate a much broader space of possible “relative phases” of the two evolving vectors. In this case, however, the effective space of states visited describes the coherent evolution of two spins at two *different* locations (the two interferometer's paths). Its dimensionality is four, as the space is spanned by the four states labeled by spin up and down in the first region, and spin up and down in the second region. Accordingly, an ex-

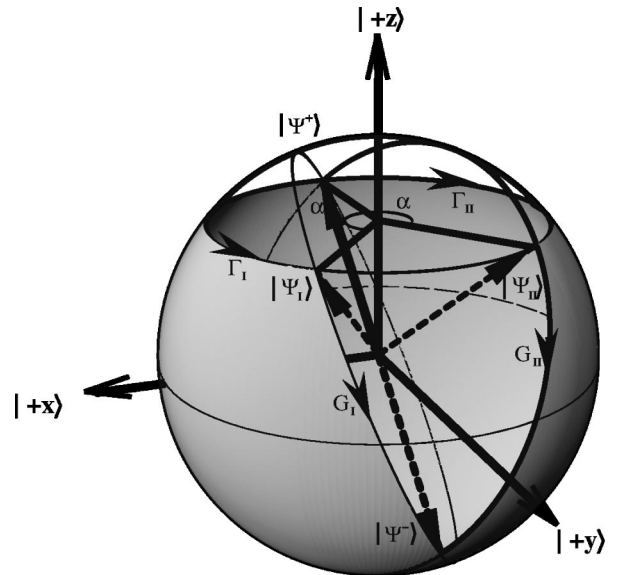


FIG. 8. Schematic representation of the spinor evolution on the spin sphere to illustrate alternative interpretation of the off-diagonal geometric phase: a combination of the geometric and dynamical parts. $|\Psi^+\rangle$ evolves to $|\Psi_I\rangle$ along the trajectory Γ_I and to $|\Psi_{II}\rangle$ along Γ_{II} and ends up at $|\Psi^-\rangle$ along the geodesic paths G_I and G_{II} . The shaded surface corresponds to the geometric part of the off-diagonal geometric phase.

periment of the kind outlined here can access a more complicated set of diagonal and off-diagonal phases, since a four-state system has a richer range of degrees of freedom than the spin-1/2 system. Obtaining satisfactory control over these phases could have potential applications in the field of quantum information.

V. CONCLUSION

In summary, we have exploited spin-polarized neutron interferometry to observe the off-diagonal geometric phase. The essential spinor evolutions were realized by the use of two spin rotators, keeping the directions of the magnetic fields antiparallel, and the polarization analysis was made after the interferometer. We built a setup insensitive to all (nongeometric) dynamical phases. Final counts with and without polarization analysis enabled us to directly observe both off-diagonal and diagonal geometric phases in two detectors for noncyclic evolutions. In particular, this experiment provides a direct quantitative measure of the off-diagonal geometric phase. The data confirm the theoretical prediction that this off-diagonal phase should remain con-

stantly equal to π in a two-state system. The combined use of the outgoing spin analysis together with the incoming polarized beam extended the range of the experimental conditions: our experimental setup permitted us to measure a wide range of phenomena, including the 4π periodicity of the spin-1/2 wave function and the noncyclic Pancharatnam phase. Furthermore, the results illustrate the significance of the off-diagonal geometric phase, especially when the diagonal geometric phase is undefined. We discussed our experiment in terms of the quantum-erasing phenomenon, where the wave property is reestablished by the modification of the path information after recombining the beam in the interferometer. We propose further directions for the investigation of geometric phases in neutron interferometry.

ACKNOWLEDGMENTS

We thank R. Gähler for providing needed equipment. This work was supported by the Austrian Fonds zur Förderung der Wissenschaftlichen Forschung (Project No. F1513) and the EU-TMR-Network “Perfect Crystal Neutron Optics” (Grant No. ERB-EMRX-CT 96-0057).

-
- [1] S. Pancharatnam, Proc. Indian Acad. Sci., Sect. A **44**, 247 (1956).
- [2] M. V. Berry, Proc. R. Soc. London, Ser. A **392**, 45 (1984).
- [3] *Geometric Phases in Physics*, edited by A. Shapere and F. Wilczek (World Scientific, Singapore, 1989).
- [4] Y. Aharonov and J. Anandan, Phys. Rev. Lett. **58**, 1593 (1987).
- [5] J. Samuel and R. Bhandari, Phys. Rev. Lett. **60**, 2339 (1988).
- [6] T. Bitter and D. Dubbers, Phys. Rev. Lett. **59**, 251 (1987).
- [7] D. J. Richardson, A. I. Kilvington, K. Green, and S. K. Lamoreaux, Phys. Rev. Lett. **61**, 2030 (1988).
- [8] J. A. Jones, V. Vedral, A. Ekert, and G. Catagnoll, Nature (London) **403**, 869 (2000).
- [9] A. Ekert, M. Ericsson, P. Hayden, H. Inamori, J. A. Jones, D. K. L. Oi, and V. Vedral, J. Mod. Opt. **47**, 2501 (2000).
- [10] J. Anandan and L. Stodolsky, Phys. Rev. D **35**, 2597 (1987).
- [11] N. Manini and F. Pistolesi, Phys. Rev. Lett. **85**, 3067 (2000).
- [12] H.-M. Lauber, P. Weidenhammer, and D. Dubbers, Phys. Rev. Lett. **72**, 1004 (1994).
- [13] F. Pistolesi and N. Manini, Phys. Rev. Lett. **85**, 1585 (2000).
- [14] V. F. Sears, *Neutron Optics* (Oxford University Press, Oxford, 1989).
- [15] H. Kaiser and H. Rauch, in *Optics of Waves and Particles*, edited by L. Bergmann and C. Schaefer (Walter de Gruyter, Berlin, 1999), Sec. 11.
- [16] *Neutron Interferometry*, edited by U. Bonse and H. Rauch (Clarendon Press, Oxford, 1979).
- [17] A. G. Klein and S. A. Werner, Rep. Prog. Phys. **46**, 259 (1983).
- [18] *Matter Wave Interferometry*, edited by G. Badurek, H. Rauch, and A. Zeilinger, special issue of Physica B **151** (1988).
- [19] H. Rauch and S. A. Werner, *Neutron Interferometry* (Clarendon Press, Oxford, 2000).
- [20] For instance, G. Badurek, H. Rauch, and J. Summhammer, in Ref. [18], p. 82.
- [21] J. Summhammer, G. Badurek, H. Rauch, U. Kischko, and A. Zeilinger, Phys. Rev. A **27**, 2523 (1983).
- [22] G. Badurek, H. Rauch, and J. Summhammer, Phys. Rev. Lett. **51**, 1015 (1983).
- [23] G. Badurek, H. Rauch, and D. Tuppinger, Phys. Rev. A **34**, 2600 (1986).
- [24] A. G. Wagh, V. C. Rakhecha, J. Summhammer, G. Badurek, H. Weinfurter, B. E. Allman, H. Kaiser, K. Hamacher, D. L. Jacobsen, and S. A. Werner, Phys. Rev. Lett. **78**, 755 (1997).
- [25] B. E. Allman, H. Kaiser, S. A. Werner, A. G. Wagh, V. C. Rakhecha, and J. Summhammer, Phys. Rev. A **56**, 4420 (1997).
- [26] A. G. Wagh, V. C. Rakhecha, P. Fischer, and A. Ioffe, Phys. Rev. Lett. **81**, 1992 (1998); R. Bhandari, *ibid.* **83**, 2089 (1999); A. G. Wagh *et al.*, *ibid.* **83**, 2090 (1999).
- [27] A. G. Wagh, G. Badurek, V. C. Rakhecha, R. J. Buchelt, and A. Schricker, Phys. Lett. A **268**, 209 (2000).
- [28] Y. Hasegawa, M. Zawisky, H. Rauch, and A. Ioffe, Phys. Rev. A **53**, 2486 (1996).
- [29] Y. Hasegawa, R. Loidl, M. Baron, G. Badurek, and H. Rauch, Phys. Rev. Lett. **87**, 070401 (2001).
- [30] G. Kroupa, G. Bruckner, O. Bolik, M. Zawisky, M. Hainbuchner, G. Badurek, R. J. Buchelt, A. Schricker, and H. Rauch, Nucl. Instrum. Methods Phys. Res. A **440**, 604 (2000).
- [31] G. Badurek, R. J. Buchelt, B.-G. Englert, and H. Rauch, Nucl. Instrum. Methods Phys. Res. A **440**, 562 (2000).
- [32] G. Badurek, R. J. Buchelt, G. Kroupa, M. Baron, and M. Villa, Physica B **283**, 389 (2000).
- [33] R. Bhandari, Phys. Lett. A **157**, 221 (1991).
- [34] For instance, M. O. Scully and K. Dühl, Phys. Rev. A **25**, 2208 (1982); A. G. Zajonc, L. J. Wang, X. Y. Zou, and L. Mandel, Nature (London) **353**, 507 (1991); P. D. D. Schwindt, P. G. Kwiat, and B.-G. Englert, Phys. Rev. A **60**, 4285 (1999).